

Dicopper Complexes with a Dissymmetric Dicompartamental Schiff Base–Oxime Ligand: Synthesis, Structure, and Magnetic Interactions

Elena V. Rybak-Akimova,[†] Daryle H. Busch,^{*,†} Pawan K. Kahol,[‡] Nicholas Pinto,[‡] Nathaniel W. Alcock,[§] and Howard J. Clase[§]

Department of Chemistry, University of Kansas, Lawrence, Kansas 66045, Department of Chemistry, Wichita State University, Wichita, Kansas 67208, and Department of Chemistry, University of Warwick, Coventry CV4 7AL, United Kingdom

Received January 31, 1996[⊗]

A dicopper(II) complex with an unsymmetrical dicompartamental ligand containing bridging phenolic oxygen atoms was synthesized by stepwise condensation, in the presence of copper(II) ions, of 2,6-diformyl-4-methylphenol and diaminopropane, followed by hydroxylamine. The complex was isolated and characterized as Cl^- , $[\text{Cu}_2\text{Cl}_4]^{2-}$, and ClO_4^- derivatives. A byproduct of the reaction, a copper(II) complex with a substituted salicylaldoxime, was also structurally characterized. The structure of the binuclear cation of major interest is nearly planar, with the copper(II) ions slightly displaced to opposite sides of the plane of the donor atoms ($<0.20 \text{ \AA}$). $[\text{Cu}_2\text{Cl}_4]^{2-}$ is an unusual anion, having been characterized previously in only five other compounds. It is flat, with both copper(I) ions in trigonal planar environments and two chlorides bridging the two copper(I) centers. X-ray structure determinations of the $[\text{Cu}_2\text{Cl}_4]^{2-}$ and ClO_4^- derivatives of the dicopper complex reveal a strong tendency for the formation of coordination dimers and tetramers. These aggregates arise because an oxime oxygen from one binuclear cationic complex coordinates axially to the copper atom of another such complex. In the case of the $[\text{Cu}_2\text{Cl}_4]^{2-}$ salt, the anion forms additional bridges between binuclear complexes, resulting in polymeric chains. In the ClO_4^- salt, however, aggregation is limited to the tetramer because of terminal axially coordinated methanol molecules. Temperature-dependent magnetic susceptibility measurements show strong antiferromagnetic interaction (*ca.* -700 cm^{-1}) between the two copper(II) ions within one binuclear cationic complex. No magnetic interactions have been observed between binuclear units. Cyclic voltammograms were measured in dimethylformamide (DMF) solution and show two separate reduction waves at -1.47 and -1.04 V , as well as an oxidation wave at $+0.04 \text{ V}$ (*vs* Fc^+/Fc). The mixed-valent $\text{Cu}^{\text{II}}/\text{Cu}^{\text{I}}$ complex is thermodynamically stable toward disproportionation.

Introduction

The rich chemistry of complexes of dicompartamental ligands binding identical metals (and to a lesser extent different metals) has been applied to the investigation of magnetic exchange interactions between the two metal ions, the stabilization of mixed-valent species, and the activation of small molecules.^{1–6} Particularly significant examples of this type are planar ligands with imine or amine donors and bridging phenolic oxygens, which are usually referred to as Robson-type ligands (**I** in Figure 1; Figure 2a).^{5,6} In these ligands, substituents X, Y, and Z can easily be varied, giving both symmetric and dissymmetric ligands. Dicopper complexes have been especially significant, because of their interesting properties and the relative simplicity of their synthesis.^{5,6} In most cases the two copper centers are strongly antiferromagnetically coupled.^{3,4,5b}

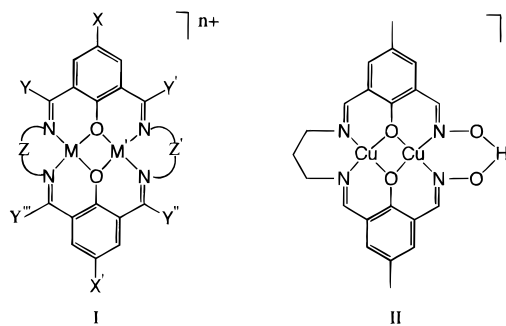


Figure 1. (I) Robson-type binuclear complex. (II) Dissymmetric complex of ligand (L) containing Schiff base and oxime compartments.

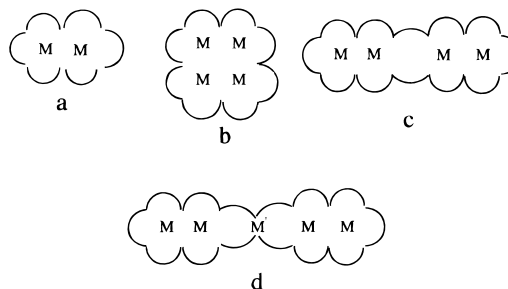


Figure 2. Different types of metal atom alignments in polynuclear complexes.

Recently, the chemistry of Robson-type complexes has been expanded by increasing the number of donor atoms in the ligands and, consequently, the number of metal ions coordinated by what are now multicompartmental ligands. For example,

[†] University of Kansas.

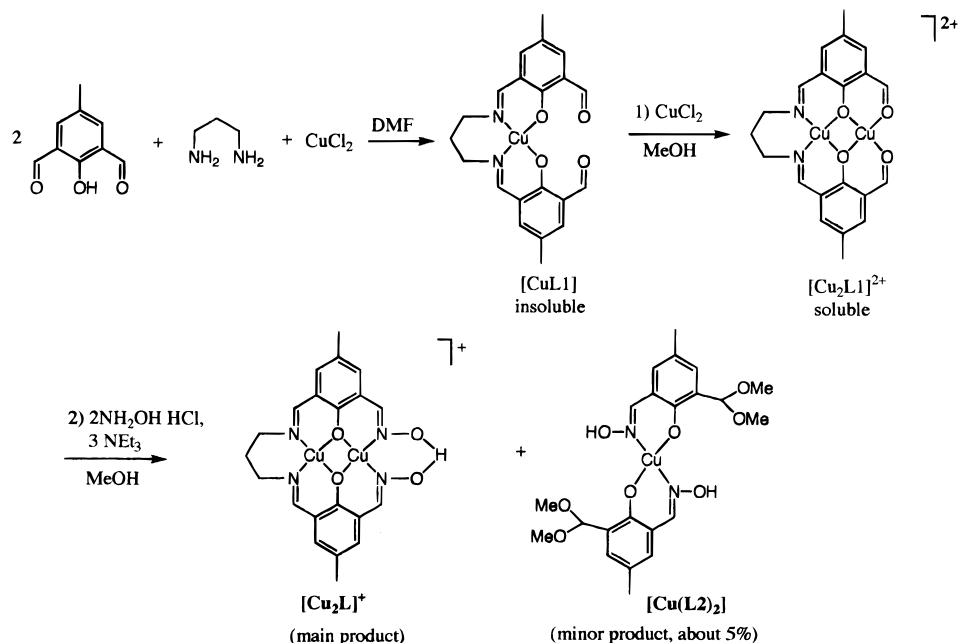
[‡] Wichita State University.

[§] University of Warwick.

[⊗] Abstract published in *Advance ACS Abstracts*, January 15, 1997.

- (1) Guerriero, P.; Tamburini, S.; Vigato, P. A. *Coord. Chem. Rev.* **1995**, *139*, 17.
- (2) Fraser, C.; Ostrander, R.; Rheingold, A. L.; White, C.; Bosnich, B. *Inorg. Chem.* **1994**, *33*, 324.
- (3) Cairns, C. J.; Busch, D. H. *Coord. Chem. Rev.* **1986**, *69*, 1. Groh, S. E. *Israel J. Chem.* **1976–1977**, *15*, 277. Zanello, P.; Tamburini, S.; Vigato, P. A.; Mazzocchin, G. A. *Coord. Chem. Rev.* **1987**, *77*, 165.
- (4) Kahn, O. *Struct. Bonding (Berlin)* **1987**, *68*, 89.
- (5) (a) Vigato, P. A.; Tamburini, S.; Fenton, D. E. *Coord. Chem. Rev.* **1990**, *106*, 25. (b) Casselato, U.; Vigato, P. A.; Fenton, D. E.; Vidali, M. *Coord. Chem. Rev.* **1979**, *8*, 199.
- (6) Atkins, A. J.; Black, D.; Blake, A. J.; Marin-Becerra, A.; Parsons, S.; Ruiz-Ramirez, L.; Schröder, M. *Chem. Commun.* **1996**, 457.

Scheme 1



complexes with four,^{7–11} six,^{12,13} eight,^{7a–c} and twelve¹² metals have been described, and some of their magnetic interactions have been characterized. In most of these compounds, however, magnetic interaction is limited to the pairs of metal ions. Thus, the cores of four-metal clusters (type b, Figure 2) are best described as “dimers of dimers”, containing pairs of magnetically coupled ions with no significant magnetic interaction between the pairs,^{9,11} despite the apparent symmetry of the simple representation of their structure. Similarly, dimers of Figure 2a type dinuclear complexes do not show significant magnetic interaction between dinuclear units.^{14,15} To the extent of our knowledge, the only example of extended magnetic interaction throughout such polynuclear complexes has been observed for a “benzene-like” cyclic array of six metal ions.¹² A more favorable situation can be expected if metal chains rather than metal cores are present in the structure. Attempts have recently been made to connect two dicompartmental Robson-

type ligands by means of an organic group,^{15,16} although the coordination chemistry of such ligands has not been extensively studied, and tetranuclear complexes of type c (Figure 2) were not obtained.

We suggest a different approach to the construction of metal chains based on Robson-type ligands, using two bimetallic units connected to each other by a fifth metal ion (type d, Figure 2). This requires dicompartmental ligands with additional donor atoms capable of coordination with the “extra” metal ion. Oxime groups are appropriate candidates, providing “external” donors in the form of their oxygen atoms, while the oxime nitrogen atoms are bound to the metal ions within a dicompartmental ligand. Some examples of polynuclear complexes with bridging oxime ligands have been reported.^{17,18} Here we report the synthesis and characterization of a binuclear building block (**II**, Figure 1) for the type d (Figure 2) complexes. Despite the asymmetric nature of the ligand, the dicopper complexes **II** (Figure 1), which are characterized in this paper, are shown to retain the advantages of symmetrical Robson-type complexes; e.g., strong antiferromagnetic coupling within a binuclear cation and stabilization of mixed-valent Cu^{II}Cu^I species toward disproportionation. The additional donors present in the oxime groups play the predicted role of bridging groups between binuclear units, giving rise to coordination tetramers or polymers.

Results and Discussion

Synthesis. We have synthesized and characterized three dicopper complexes of an asymmetric ligand containing a Schiff

- (7) (a) McKee, V.; Tandon, S. S. *J. Chem. Soc., Chem. Commun.* **1988**, 385. (b) McKee, V.; Tandon, S. S. *Inorg. Chem.* **1989**, 28, 2901. (c) McKee, V.; Tandon, S. S. *J. Chem. Soc., Dalton Trans.* **1991**, 221. (d) McKee, V.; Tandon, S. S. *J. Chem. Soc., Chem. Commun.* **1988**, 1334.
- (8) Nanda, K. K.; Venkatsubramanian, K.; Majumdar, D.; Nag, K. *Inorg. Chem.* **1994**, 33, 1581.
- (9) Sakijama, H.; Tokuyama, K.; Matsumura, Y.; Ōkawa, H. *J. Chem. Soc., Dalton Trans.* **1993**, 2329.
- (10) Motoda, K.-i.; Sakijama, H.; Matsumoto, N.; Ōkawa, H.; Fenton, D. E. *J. Chem. Soc., Dalton Trans.* **1995**, 3419. Sakijama, H.; Motoda, K.; Ōkawa, H.; Kida, S. *Chem. Lett.* **1991**, 1133.
- (11) Edwards, A. J.; Hoskins, B. F.; Robson, R.; Wilson, J. C.; Moubaraki, B.; Murray, K. S. *J. Chem. Soc., Dalton Trans.* **1994**, 1837. Grannas, M. J.; Hoskins, B. F.; Robson, R. *Inorg. Chem.* **1994**, 33, 1071. Edwards, A. J.; Hoskins, B. F.; Kachab, E. H.; Markiewicz, A.; Murray, K. S.; Robson, R. *Inorg. Chem.* **1992**, 31, 3585. Bell, M.; Edwards, A. J.; Hoskins, B. F.; Kachab, E. H.; Robson, R. *J. Am. Chem. Soc.* **1989**, 111, 3603. Bell, M.; Edwards, A. J.; Hoskins, B. F.; Kachab, E. H.; Robson, R. *J. Chem. Soc., Chem. Commun.* **1987**, 1852.
- (12) Tandon, S. S.; Thompson, L. K.; Bridson, J. N.; Benelli, C. *Inorg. Chem.* **1995**, 34, 5507. Tandon, S. S.; Thompson, L. K.; Bridson, J. N. *J. Chem. Soc., Commun.* **1992**, 911.
- (13) Hoskins, B. F.; Robson, R.; Smith, P. J. *J. Chem. Soc., Chem. Commun.* **1990**, 488.
- (14) Tandon, S. S.; Thompson, L. K.; Bridson, J. N.; McKee, V.; Downard, A. J. *Inorg. Chem.* **1992**, 31, 4635.
- (15) Tandon, S. S.; Thompson, L. K.; Bridson, J. N.; Bubenik, M. *Inorg. Chem.* **1993**, 32, 4621.

- (16) Tandon, S. S.; Thompson, L. K.; Bridson, J. N. *Inorg. Chem.* **1993**, 32, 32. Perez, M. A.; Bermejo, J. M. *An. Quim.* **1993**, 89, 105. Perez, M. A.; Bermejo, J. M. *J. Org. Chem.* **1993**, 58, 2628.
- (17) Krebs, C.; Winter, M.; Weyhermüller, T.; Bill, E.; Wieghardt, K.; Chaudhuri, P. *J. Chem. Soc., Chem. Commun.* **1995**, 1913. Colacio, E.; Dominguez-Vera, J. M.; Escuer, A.; Kivekas, R.; Romero, A. *Inorg. Chem.* **1994**, 33, 3914. Birkelbach, F.; Winter, M.; Florke, U.; Haupt, H.-J.; Butzlaff, C.; Lengen, M.; Bill, E.; Trautwein, A. X.; Wieghardt, K.; Chaudhuri, P. *Inorg. Chem.* **1994**, 33, 3990. Ruiz, R.; Lloret, F.; Julve, M.; Munoz, M. C.; Bois, C. *Inorg. Chim. Acta* **1994**, 219, 179. Shiozuka, M.; Matsumoto, N.; Ōkawa, H. *Bull. Chem. Soc. Jpn.* **1992**, 67, 1988.
- (18) Lineau, D.; Oshio, H.; Ōkawa, H.; Kida, S. *J. Chem. Soc., Dalton Trans.* **1990**, 2283.

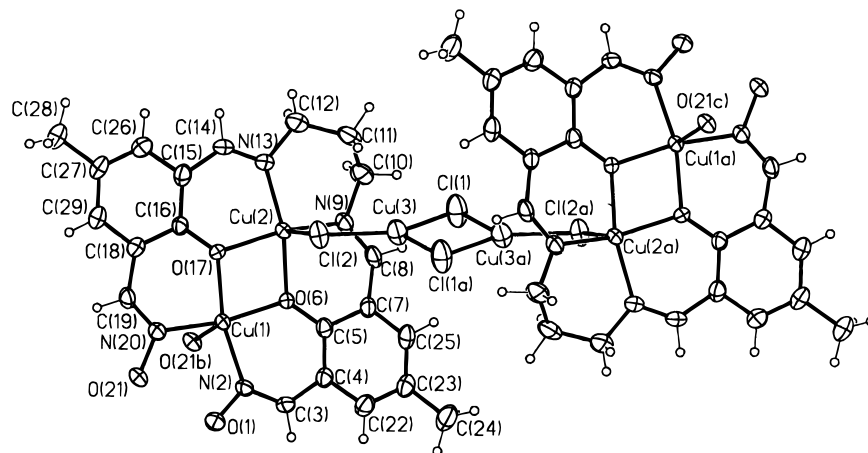


Figure 3. Crystal structure of $[\text{Cu}_2\text{L}]_2[\text{Cu}_2\text{Cl}_4]$: front view of one dicopper cation, showing atomic numbering.

base fragment on one side and two oxime groups on the other (**II**, Figure 1). The complexes contain the same cation $[\text{Cu}_2\text{L}]^+$ and different anions, chloride perchlorate, and $[\text{Cu}_2\text{Cl}_4]^{2-}$. Perchlorate anion is not coordinated to the binuclear cation, the $\text{Cu}_2\text{Cl}_4^{2-}$ is bound to the Cu(II) in the binuclear cation through chloride bridges in the solid complex, and the coordination mode of Cl^- in the chloride derivative has not been studied (see the discussion of the structures below). The ligand L has two different compartments, so a two-step synthesis was used for the dicopper complex (Scheme 1). A similar approach has previously been used to make other dicopper complexes with unsymmetrical ligands.^{2,19–22}

The product of the first step, CuL1 , is insoluble in most common organic solvents, and because this interferes with the subsequent reaction, the dicopper complex was chosen to build the oxime coordination compartment of the complex. In this process the next step involves addition of a second copper atom to give a soluble intermediate. After incorporation of the second copper(II) ion into an empty compartment, the coordinated aldehydes were transformed into oxime groups by condensation with hydroxylamine. The reactions of metal complexes have been widely used to make macrocyclic complexes, but they are not generally employed in the synthesis of complexes with oxime ligands, where the ligand is usually prepared prior to complex formation. Our example demonstrates that the metal ion promoted synthesis of oxime complexes can compete with traditional methods.

In the case of polyfunctional compounds, the main reaction, condensation of hydroxylamine with the free aldehyde groups present in $[\text{Cu}_2\text{L1}]^{2+}$, is accompanied by a parallel reaction in which azomethine bonds of the preformed Schiff base are cleaved, apparently with the replacement of diaminopropane by hydroxylamine. As a result, an unexpected byproduct, $[\text{Cu}(\text{L}_2)_2]$ (Scheme 1), a copper(II) complex with two substituted salicylaldoxime fragments, was isolated in a crystalline form. The high reactivity of aldehyde and/or azomethine groups toward substitution reactions is confirmed by the easy formation of acetals; the dimethylacetal groups in $\text{Cu}(\text{L}_2)_2$ were formed under mild reaction conditions, by reaction with the solvent methanol.

The main product of the reaction (Scheme 1) precipitates in the form of $[\text{Cu}_2\text{L}]\text{Cl}$. It is accompanied by a small amount of

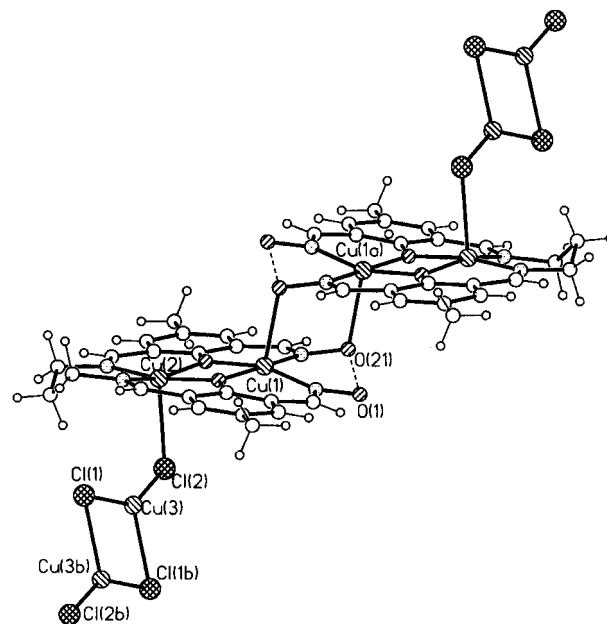


Figure 4. Crystal structure of $[\text{Cu}_2\text{L}]_2[\text{Cu}_2\text{Cl}_4]$: side view of the complex, showing the linkage into chains through oxime and anion bridges.

the complex with a different anion ($[\text{Cu}_2\text{Cl}_4]^{2-}$). This copper(I) anion is probably formed by the reduction of copper(II) by hydroxylamine, and the yield of the tetrachlorodicuprate(I) salt can be increased if one extra equivalent each of copper(II) chloride and of hydroxylamine hydrochloride is used in the second reaction step. The perchlorate salt was also obtained, by the addition of NaClO_4 to a solution of the chloride derivative. *Caution: perchlorate salts are often explosive.*

Characterization. The synthesized binuclear complexes were characterized by elemental analysis (including Cu analysis), mass spectrometry (positive FAB), IR and electronic spectroscopy and, for three compounds, by crystal structure determination. The main peak in the mass spectrum of each complex corresponds to the molecular ion $[\text{Cu}_2\text{L}]^+$ with the isotopic pattern characteristic of a dicopper compound. The IR spectra support the reactions shown in Scheme 1; the spectra of all three salts look similar, and the frequencies for $[\text{Cu}_2\text{L}]_2[\text{Cu}_2\text{Cl}_4]$ are cited here. The carbonyl stretch present at 1670 cm^{-1} in the IR of the precursor $[\text{CuL1}]^{21,23}$ disappears in the spectrum of $[\text{Cu}_2\text{L}]^+$. The $\text{C}=\text{N}$ stretch of the new azomethine bond in the

(19) Fraser, C.; Bosnich, B. *Inorg. Chem.* **1994**, *33*, 338.

(20) Karunakaran, S.; Kandaswamy, M. *J. Chem. Soc., Dalton Trans.* **1994**, 1595.

(21) Okawa, H.; Kida, S. *Bull. Chem. Soc. Jpn.* **1972**, *45*, 1759.

(22) Casellato, U.; Fregona, D.; Sitran, S.; Tamburini, S.; Vigato, P. A. *Inorg. Chim. Acta* **1985**, *110*, 181.

(23) Gagné, R. R.; Spiro, C. L.; Smith, T. J.; Hamann, C. A.; Thies, W. R.; Shiemke, A. K. *J. Am. Chem. Soc.* **1981**, *103*, 4073.

Table 1. Crystallographic Data

	[Cu ₂ L] ₂ ⁺ [Cu ₂ Cl ₄] ²⁻ (A)	[Cu ₂ L] ₄ ⁺ [ClO ₄] ₄ ⁻ ·4MeOH (B)	[Cu(L ₂) ₂] (C)
formula	[C ₂₁ H ₂₁ Cu ₂ N ₄ O ₄] ₂ ⁺ [Cu ₂ Cl ₄] ²⁻	[C ₈₈ H ₁₀₀ Cu ₈ N ₁₆ O ₂₀] ₄ ⁺ [ClO ₄] ₄ ⁻	C ₂₂ H ₂₈ CuN ₂ O ₈
M _r	653.93	2608.04	512.0
syst	triclinic	triclinic	monoclinic
space group	P $\bar{1}$	P $\bar{1}$	P2 ₁ /c
a/Å	8.0452(11)	8.637(7)	12.273(5)
b/Å	8.7160(10)	15.875(11)	11.790(7)
c/Å	16.913(2)	19.44(2)	8.048(5)
α/deg	96.471(9)	106.51(6)	90
β/deg	93.088(8)	97.50(7)	97.41(4)
γ/deg	105.273(10)	96.77(6)	90
U/Å ³	1132.4(2)	2499(4)	1154.8(11)
Z	1	1	2
D(calc)/(g cm ⁻³)	1.918	1.733	1.472
T/K	295(2)	293(2)	293(2)
cryst. dimens/mm	0.84 × 0.21 × 0.092	0.06 × 0.10 × 0.18	0.40 × 0.22 × 0.11
wavelength, Å	0.709 26	0.709 26	0.709 26
μ(Mo Kα)/mm ⁻¹	3.066	1.869	0.996
R1(obs F) ^a	0.037	0.0541	0.052
R2 _w (all F ²) ^a	0.100	0.141	0.141

^a R indices based on F² are denoted R2 and those based on F are denoted R1, e.g., R2_w = [Σ[w(F_o² - F_c²)²]/Σ[w(F_o²)²]^{1/2} and R1 = Σ||F_o - |F_c||/Σ|F_o|.

oxime fragment probably overlaps with that of the Schiff base fragment, since only one strong band is observed at 1628 cm⁻¹ in the spectrum of [Cu₂L]⁺. Two N–O bands (characteristic for oxime complexes and usually observed at 1060–1250 cm⁻¹) appear in the spectrum of [Cu₂L]⁺ after the completion of the second step in Scheme 1: a new band appears at 1192 cm⁻¹, and three absorptions are observed in the spectrum of [Cu₂L]⁺ at 1068, 1097, and 1115 cm⁻¹, while only two bands are present in the same region in the spectrum of [CuL1] (at 1082 and 1107 cm⁻¹). A weak feature sometimes observed for oxime complexes in the region between 2300 and 2700 cm⁻¹, and attributed to the hydrogen-bonded fragment O–H–O,²⁴ is not present in the spectra of our complexes. Strong bands at 1090 and 625 cm⁻¹ in the spectrum of the perchlorate salt are due to that anion.

The electronic spectra of [Cu₂L]Cl and [Cu₂L]₂[Cu₂Cl₄], measured in methanol solutions in the range 330–1200 nm, are very similar. The chloride derivative gave the following λ_{max} (ε) values (extinction coefficients per one complex cation): 385 (3300), 600 (broad, 120), 700 sh (ca. 80), 945 (25), 1150 (20) nm. For the tetrachlorodocuprate(I) complex, very similar spectra were recorded: 395 (2700), 610 (broad, 110), 700 sh (ca. 80), 945 (53), 1150 (73) nm. For dicopper complexes with Robson-type ligands, an intense band in the near-UV region is usually assigned to an intraligand transition of the C=N fragment overlapping with a copper–phenolic oxygen charge transfer transition, while a moderate band at about 600 nm is assigned to d–d transitions.^{14,19–21,25–32} The latter band is sometimes less broad and more intense than that observed for our asymmetric complex. It might be suggested

that, in our complex, the copper ions in the oxime and Schiff base compartments are not equivalent and absorb at slightly different energies. However, almost the same ligand-field spectrum was observed for a symmetrical analog of [Cu₂L]⁺ (Figure 1, X = Me, Y = H, Z = (CH₂)₃): 600 nm (90), 700(sh) nm (60).^{25,27} An explanation for this spectrum (as well as an alternative explanation for the spectrum of [Cu₂L]⁺) requires the Cu(II) ions to be five-coordinated, since two bands are usually observed at similar wavelengths for five-coordinated copper complexes, with the high-energy band more intense than the low-energy one.³³ A remarkable feature of the spectrum of [Cu₂L]₂[Cu₂Cl₄] is its significant absorbance in the near-IR region, which can be tentatively assigned to near-IR d–d bands in tetragonal-pyramidal Cu(II) complexes.³³

Crystal Structures. (A) [Cu₂L][Cu₂Cl₄] The dicopper complex cation with the asymmetric Schiff base–oxime ligand is planar, with the copper(II) ions slightly displaced to opposite sides of the plane of the donor atoms (0.19 Å for the Schiff base compartment and 0.16 Å for the oxime compartment) (Figures 3 and 4). The Cu–N and Cu–O distances are comparable with those in analogous complexes,^{1,2,7a–c,14,28,34–43} with slightly shorter bond lengths in the oxime compartment than on the Schiff base side (Table 2). The copper–copper separation is 3.07 Å. The bridging angles Cu–O(Ph)–Cu within the binuclear cation are equal to 103.17(8)° (Cu(1)–O(6)–Cu(2)) and 102.29(8)° (Cu(1)–O(17)–Cu(2)). The ge-

(24) Egneus, B. *Talanta* **1972**, *19*, 1387. Burger, K.; Ruff, I.; Ruff, F. J. *Inorg. Nucl. Chem.* **1965**, *27*, 179.

(25) Pilkington, N. H.; Robson, R. *Aust. J. Chem.* **1970**, *23*, 2225.

(26) Gagné, R. R.; Koval, C. A.; Smith, T. J. *J. Am. Chem. Soc.* **1977**, *99*, 8367.

(27) Mandal, S. K.; Nag, K. *J. Chem. Soc., Dalton Trans.* **1983**, 2429.

(28) Mandal, S. K.; Thompson, L. K.; Nag, K.; Charland, J.-P.; Gabe, E. *J. Inorg. Chem.* **1987**, *26*, 1391.

(29) Gagné, R. R.; Koval, C. A.; Smith, T. J.; Cimolino, M. C. *J. Am. Chem. Soc.* **1979**, *101*, 4571.

(30) (a) Okawa, H.; Nishio, J.; Ohba, M.; Tadokoro, M.; Matsumoto, N.; Koikawa, M.; Kida, S.; Fenton, D. E. *Inorg. Chem.* **1993**, *32*, 2949. (b) Okawa, H.; Tadokoro, M.; Aratake, Y.; Ohba, M.; Shindo, K.; Mitsumi, M.; Koikawa, M.; Tomono, M.; Fenton, D. E. *J. Chem. Soc., Dalton Trans.* **1993**, 253.

(31) Long, R. C.; Hendrickson, D. N. *J. Am. Chem. Soc.* **1983**, *105*, 1513.

(32) Mandal, S. K.; Nag, K. *J. Chem. Soc., Dalton Trans.* **1984**, 2141.

(33) Lever, A. B. P. *Inorganic Electronic Spectroscopy*; Elsevier: Amsterdam, 1984.

(34) Lacroix, P.; Kahn, O.; Gleizes, A.; Valade, L.; Cassoux, P. *Nouv. J. Chim.* **1984**, *8*, 643.

(35) Lacroix, P.; Kahn, O.; Theobald, F.; Leroy, J.; Wakselman, C. *Inorg. Chim. Acta* **1988**, *142*, 129.

(36) Gagné, R. R.; Henling, L. M.; Kistenmacher, T. J. *Inorg. Chem.* **1980**, *19*, 1226.

(37) Hoskins, B. F.; McLeod, N. J.; Schaap, H. A. *Aust. J. Chem.* **1976**, *29*, 515.

(38) Mandal, S. K.; Thompson, L. K.; Nag, K.; Charland, J.-P.; Gabe, E. *J. Can. J. Chem.* **1987**, *65*, 2815.

(39) Mandal, S. K.; Thompson, L. K.; Newlands, M. J.; Gabe, E. J.; Nag, K. *Inorg. Chem.* **1990**, *29*, 1324.

(40) Mandal, S. K.; Thompson, L. K.; Newlands, M. J.; Gabe, E. J. *Inorg. Chem.* **1989**, *28*, 3707.

(41) Carlisle, W. D.; Fenton, D. E.; Roberts, P. B.; Casellato, U.; Vigato, P. A.; Graziani, R. *Transition Met. Chem.* **1986**, *11*, 292.

(42) Brychey, K.; Drager, K.; Jens, K.-J.; Tilset, M.; Behrens, U. *Chem. Ber.* **1994**, *127*, 465.

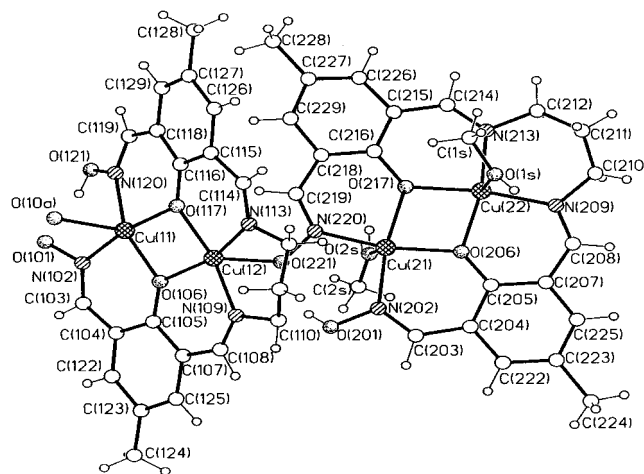
(43) Brychey, K.; Drager, K.; Jens, K.-J.; Tilset, M.; Behrens, U. *Chem. Ber.* **1994**, *127*, 1817.

Table 2. Selected Bond Lengths (Å) and Angles (deg)

(i) For $[\text{Cu}_2\text{L}]_2^+[\text{Cu}_2\text{Cl}_4]^{2-}$ (A) ^a			
Cu(1)—N(20)	1.947(2)	Cu(2)—O(17)	1.996(2)
Cu(1)—N(2)	1.955(2)	Cu(2)—Cl(2)	2.6462(9)
Cu(1)—O(17)	1.958(2)	Cu(3)—Cl(1)	2.2115(11)
Cu(1)—O(6)	1.960(2)	Cu(3)—Cl(2)	2.1516(9)
Cu(1)—O(21) ¹	2.388(2)	Cu(3)—Cl(1) ²	2.4664(11)
Cu(2)—N(13)	1.965(2)	Cu(3)—Cu(3) ²	2.9937(10)
Cu(2)—O(6)	1.971(2)	Cl(1)—Cu(3) ²	2.4664(11)
Cu(2)—N(9)	1.972(2)		
N(20)—Cu(1)—N(2)	96.43(9)	O(6)—Cu(2)—O(17)	76.65(7)
N(20)—Cu(1)—O(17)	92.57(8)	N(9)—Cu(2)—O(17)	161.92(9)
N(2)—Cu(1)—O(17)	162.42(9)	Cu(1)—O(6)—Cu(2)	103.17(8)
N(20)—Cu(1)—O(6)	169.94(8)	Cu(1)—O(17)—Cu(2)	102.29(8)
N(2)—Cu(1)—O(6)	92.16(8)	N(13)—Cu(2)—Cl(2)	97.20(8)
O(17)—Cu(1)—O(6)	77.79(7)	O(6)—Cu(2)—Cl(2)	90.38(6)
N(20)—Cu(1)—O(21) ¹	88.43(8)	N(9)—Cu(2)—Cl(2)	99.02(7)
N(2)—Cu(1)—O(21) ¹	91.66(8)	O(17)—Cu(2)—Cl(2)	95.03(6)
O(17)—Cu(1)—O(21) ¹	103.69(7)	Cl(2)—Cu(3)—Cl(1)	142.75(5)
O(6)—Cu(1)—O(21) ¹	96.57(7)	Cl(2)—Cu(3)—Cl(1) ²	116.48(4)
N(13)—Cu(2)—O(6)	166.85(9)	Cl(1)—Cu(3)—Cl(1) ²	100.63(4)
N(13)—Cu(2)—N(9)	97.50(10)	Cu(3)—Cl(1)—Cu(3) ²	79.37(4)
O(6)—Cu(2)—N(9)	91.87(8)	Cu(3)—Cl(2)—Cu(2)	108.49(4)
N(13)—Cu(2)—O(17)	91.94(8)		
(ii) For $[\text{Cu}_2\text{L}]^+[\text{ClO}_4]^- \cdot \text{MeOH}$ (B) ^b			
Cu(11)—N(102)	1.928(7)	Cu(21)—N(220)	1.950(7)
Cu(11)—O(117)	1.955(5)	Cu(21)—N(202)	1.954(7)
Cu(11)—O(106)	1.961(6)	Cu(21)—O(217)	1.963(5)
Cu(11)—N(120)	1.977(7)	Cu(21)—O(206)	1.967(5)
Cu(11)—O(101) ³	2.319(6)	Cu(21)—O(2S)	2.344(7)
Cu(12)—N(113)	1.962(8)	Cu(22)—N(213)	1.961(7)
Cu(12)—O(106)	1.971(6)	Cu(22)—N(209)	1.964(7)
Cu(12)—O(117)	1.975(6)	Cu(22)—O(217)	1.976(5)
Cu(12)—N(109)	1.980(7)	Cu(22)—O(206)	1.9962(6)
Cu(12)—O(221)	2.269(6)	Cu(22)—O(1S)	2.406(7)
N(102)—Cu(11)—O(117)	170.0(3)	N(220)—Cu(21)—N(202)	97.2(3)
N(102)—Cu(11)—O(106)	93.9(3)	N(220)—Cu(21)—O(217)	92.5(3)
O(117)—Cu(11)—O(106)	77.2(2)	N(202)—Cu(21)—O(217)	170.3(3)
N(102)—Cu(11)—N(120)	96.2(3)	N(220)—Cu(21)—O(206)	166.8(3)
O(117)—Cu(11)—N(120)	91.0(3)	N(202)—Cu(21)—O(206)	92.4(3)
O(106)—Cu(11)—N(120)	159.7(2)	O(217)—Cu(21)—O(206)	77.9(2)
N(102)—Cu(11)—O(101) ³	91.7(2)	N(220)—Cu(21)—O(2S)	94.1(3)
O(117)—Cu(11)—O(101) ³	95.0(2)	N(202)—Cu(21)—O(2S)	94.4(3)
O(106)—Cu(11)—O(101) ³	105.6(2)	O(217)—Cu(21)—O(2S)	85.8(3)
N(120)—Cu(11)—O(101) ³	91.7(3)	O(206)—Cu(21)—O(2S)	94.1(3)
N(113)—Cu(12)—O(106)	163.0(3)	N(213)—Cu(22)—N(209)	97.5(3)
N(113)—Cu(12)—O(117)	91.9(3)	N(213)—Cu(22)—O(217)	93.0(3)
O(106)—Cu(12)—O(117)	76.5(2)	N(209)—Cu(22)—O(217)	169.5(3)
N(113)—Cu(12)—N(109)	98.3(3)	N(213)—Cu(22)—O(206)	168.0(3)
O(106)—Cu(12)—N(109)	91.8(3)	N(209)—Cu(22)—O(206)	92.6(3)
O(117)—Cu(12)—N(109)	167.3(3)	O(217)—Cu(22)—O(206)	77.0(2)
N(113)—Cu(12)—O(221)	98.1(3)	N(213)—Cu(22)—O(1S)	96.3(3)
O(106)—Cu(12)—O(221)	96.4(2)	N(209)—Cu(22)—O(1S)	89.6(2)
O(117)—Cu(12)—O(221)	101.8(2)	O(217)—Cu(22)—O(1S)	89.6(2)
N(109)—Cu(12)—O(221)	84.3(3)	O(206)—Cu(22)—O(1S)	90.3(2)
Cu(11)—O(106)—Cu(12)	103.1(3)	Cu(21)—O(206)—Cu(22)	102.2(3)
Cu(11)—O(117)—Cu(12)	103.2(3)	Cu(21)—O(217)—Cu(22)	102.9(3)
Cu(11)—O(117)—Cu(12)	103.2(3)		
(iii) For $[\text{Cu}(\text{L}_2)_2]$ (C) ^c			
Cu(1)—O(6)	1.865(3)	C(5)—O(6)	1.323(5)
Cu(1)—N(2)	1.946(4)	C(8)—O(9)	1.399(5)
O(1)—N(2)	1.401(4)	C(8)—O(10)	1.417(5)
N(2)—C(3)	1.289(5)		
O(6) ⁴ —Cu(1)—N(2)	88.14(14)	C(3)—N(2)—Cu(1)	127.9(3)
O(6)—Cu(1)—N(2)	91.86(14)	O(1)—N(2)—Cu(1)	119.1(3)
C(3)—N(2)—O(1)	113.0(3)	C(5)—O(6)—Cu(1)	129.1(3)

^a Symmetry transformations used to generate equivalent atoms (indicated by superscript 1 or 2): (1) $-x, -y + 1, -z + 1$; (2) $-x, -y, -z$. ^b Symmetry transformations used to generate equivalent atoms (indicated by superscript 3): $-x, -y + 2, -z$. ^c Symmetry transformations used to generate equivalent atoms (indicated by superscript 4): $-x + 1, -y + 1, -z$.

ometry of both copper ions is square-pyramidal, each forming an elongated fifth bond, either to an oxime oxygen of a different

**Figure 5.** Crystal structure of $[\text{Cu}_2\text{L}][\text{ClO}_4] \cdot \text{MeOH}$ dimer, showing atomic numbering:

ligand (2.388(2) Å) or a chloride (2.6462(9) Å). The structure is generally similar to those of analogous complexes with Robson-type dicompartmental ligands, but the present complex is the first with unsymmetrical ligands (with the exception of the Bosnich ligand which, despite containing compartments designed for six- and four-coordination, gives rise to two five-coordinate Cu ions in its dicopper complex²).

The coordinated chloride is part of the complex $[\text{Cu}_2\text{Cl}_4]^{2-}$ anion. This is an unusual anion, only previously characterized in five other compounds,^{14,44} and, significantly, two of these contain complex cations resembling that in the present example. The $[\text{Cu}_2\text{Cl}_4]^{2-}$ anion is flat, with both copper(I) ions in trigonal planar environments and two chlorides bridging the two Cu(I) centers. The anion has a center of inversion, though the CuCl_3 units are not symmetrical, their Cu—Cl distances differing by 0.5 Å.

The $[\text{Cu}_2\text{Cl}_4]^{2-}$ anion bridges two $[\text{Cu}_2\text{L}]^+$ cations, and the oxime—copper link to the other copper produces a chain structure (Figure 4), with the Cu—O(oxime)—N(oxime) angle equal to 108.5(2)°. Somewhat similar interactions have been observed for other dioxime complexes, *e.g.*, that of copper(II) with dimethylglyoxime.⁴⁵ A few Robson-type complexes are also known in which one ligand appears to be axially coordinated to the copper ion in another ligand. For example, a benzene ring is situated 2.55 and 3.04 Å above the copper(I) in one example,³⁶ while in others the oxo group from a μ -oxotetrameric cation is axially coordinated to the copper ion in the next ligand^{7a-c} or the phenolic oxygen is axially coordinated to Cu(II).^{30a} These two trends (the dimerization of copper(II) oximes and stack formation by means of axial coordination for Robson-type complexes) clearly favor the formation of dimers for oxime-containing, Robson-type complexes.

(B) $[\text{Cu}_2\text{L}][\text{ClO}_4] \cdot \text{MeOH}$. Four dinuclear cations, similar to that just described, are linked in a centrosymmetric tetramer by axial coordination of oxime oxygens to copper(II) ions (Figures 5 and 6). The geometry of all copper(II) centers is square-pyramidal, with the elongated fifth bonds to axially coordinated methanol molecules (in “terminal” cations) or oxime oxygens (in “central” cations). The terminal axially-coordinated methanol molecules prevent the formation of a polymeric chain.

(44) Banci, L.; Bencini, A.; Dei, A.; Gatteschi, D. *Inorg. Chim. Acta* **1984**, *84*, L11. Haasnoot, J. G.; Favre, T. L. F.; Hinrich, W.; Reedijk, J. *Angew. Chem., Int. Ed. Engl.* **1988**, *27*, 856. Andersson, S.; Hakansson, M.; Jagner, S. *Inorg. Chim. Acta* **1993**, *209*, 195. Escriche, L.; Lucena, N.; Casabo, J.; Teixidor, F.; Kivekas, R.; Sillanpaa, R. *Polyhedron* **1995**, *14*, 649.

(45) Vacigao, A.; Zambonelli, L. *J. Chem. Soc. A* **1970**, 218.

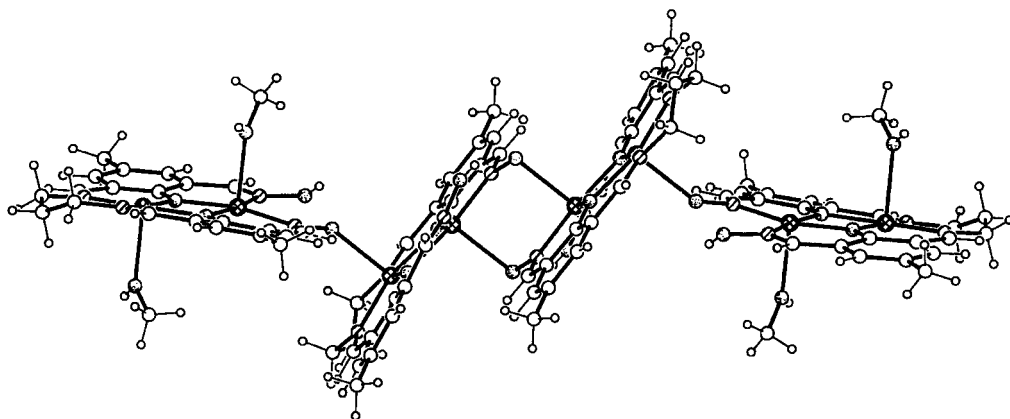


Figure 6. Crystal structure of [Cu₂L][ClO₄]·MeOH: side view of the tetrameric structure.

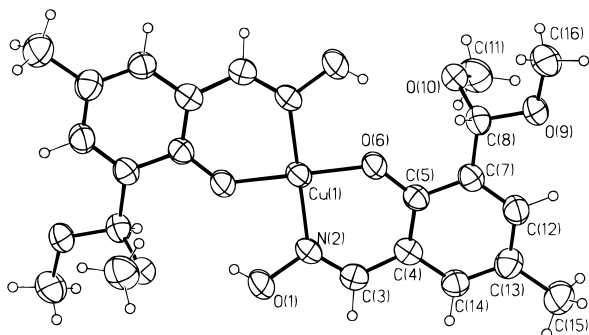


Figure 7. Crystal structure of a byproduct [Cu(L₂)₂].

The existence of this tetrameric structure in the absence of bridging anions demonstrates that coordination of oxime oxygen to copper ions alone is enough for cation aggregation. The coordination modes of the copper(II) ions are similar to those in Figure 3, but the relative nonplanarity (as compared to compound **A**) of the individual units is notable (Figure 6). However, the deviations of the Cu(II) ions from N₂O₂ plane are reasonably small: 0.195 Å (Cu(11)) and 0.165 Å (Cu(12)) for central compartments (values very close to those for the polymeric tetrachlorodicuprite salt); 0.078 Å (Cu(21)) and 0.055 Å (Cu(22)). The Cu–Cu separation in both terminal and central cations is 3.08 Å. The Cu–O(Ph)–Cu angles are as follows: 103.2(3)° (Cu(11)–O(117)–Cu(12)) and 103.1(3)° (Cu(11)–O(106)–Cu(12)) for the central cation; 102.2(3)° (Cu(21)–O(206)–Cu(22)) and 102.9(3)° (Cu(21)–O(217)–Cu(22)) for the terminal cation. The bond angle Cu–O(oxime)–N(oxime) is 130.3(5)° for central–terminal cations and 108.4(4)° for central–central cations.

(C) [Cu(L₂)₂]. This mononuclear compound is a copper(II) complex with two substituted salicylaldoxime-like anionic ligands (Figure 7). The Cu(II) ion is located in a square-planar environment, with two phenolate oxygens and two oxime nitrogens coordinated in a trans-geometry. The two functional groups of the ligand that are not bound to the metal ion have been converted into dimethylacetal groups, and there is no oxime oxygen bridging. Selected bond lengths and angles are listed in Table 2.

Magnetic Measurements. For planar Robson-type dicopper complexes, strong antiferromagnetic interactions have usually been reported.^{14,25,28,30a,34,35,38–43,46,47} However, in several cases, especially for complexes with asymmetric ligands of distorted geometry, only weak antiferromagnetic interactions were

observed.^{20,30b,43,48} To produce extensively coupled polynuclear magnetic materials on the basis of Robson-type ligands, it is important to modify the ligands in a way which will provide additional opportunities for building extended networks of magnetically coupled centers. At the same time, such modifications should not destroy the strong coupling within binuclear building blocks, which could accompany the introduction of asymmetry into the ligand. For this reason, it is important to find out whether or not the asymmetric Schiff base–oxime ligand environment supports strong antiferromagnetic interaction between two copper(II) centers. The compound [Cu₂L]₂[Cu₂Cl]₄ has a crystal structure which appears to be favorable for antiferromagnetic exchange, because it is very similar to the structure of symmetrical Robson complexes where strong antiferromagnetic interaction does occur.^{37,39,40} The structure of the cation in the chloride derivative of the dicopper complex is presumably similar to that of the binuclear cation in the tetrachlorodicuprate(I) complex. Electronic non-equivalency of two copper centers might, however, decrease the exchange coupling between them.^{3,4} The experimentally determined room temperature magnetic moments for both the chloride and tetrachlorodicuprite derivatives of the new asymmetric Schiff base–oxime dicopper complex are practically the same (0.65 B.M. per copper ion) and indicate antiferromagnetic coupling.

A cryomagnetic study was undertaken to determine the values of coupling constants, with the results shown in Figure 8. The measurements covered the temperature range from 80 to 450 K for [Cu₂L]Cl (Figure 8a) and from 5 to 450 K for [Cu₂L]₂[Cu₂Cl]₄ (Figure 8b). The behavior of the two complexes below room temperature is very similar. The data for [Cu₂L]Cl, measured over the temperature range 80–300 K, were fitted to the Bleaney-Bowers expression⁴⁹

$$\chi_m = (1 - x_p)\chi_{BB} + \left(\frac{Ng^2\beta^2}{3k_B T}\right)S(S+1)x_p + N\alpha$$

$$\chi_{BB} = \frac{Ng^2\beta^2}{k_B(T-\theta)} \left[3 + \exp\left(-\frac{2J}{k_B T}\right) \right]^{-1} \quad (1)$$

using the isotropic Heisenberg exchange Hamiltonian $H = -2JS_1S_2$ for two interacting spins equal to $-1/2$. χ_m in the above equation is expressed as emu/mole Cu, $N\alpha$ is the temperature independent paramagnetism, x_p denotes the contribution due to monomeric impurity spins, and θ is a Weiss-like correction term to account for possible magnetic interactions between spin pairs or dimers.

(46) Mandal, S. K.; Thompson, L. K.; Nag, K. *Inorg. Chim. Acta* **1988**, *149*, 247.

(47) Lambert, S. L.; Hendrickson, D. N. *Inorg. Chem.* **1979**, *18*, 2683.

(48) Timken, M. D.; Marritt, W. A.; Hendrickson, D. N.; Gagne, R. A.; Sinn, E. *Inorg. Chem.* **1985**, *24*, 4202.

(49) Bleaney, B.; Bowers, K. D. *Proc. R. Soc. London A* **1952**, *214*, 451.

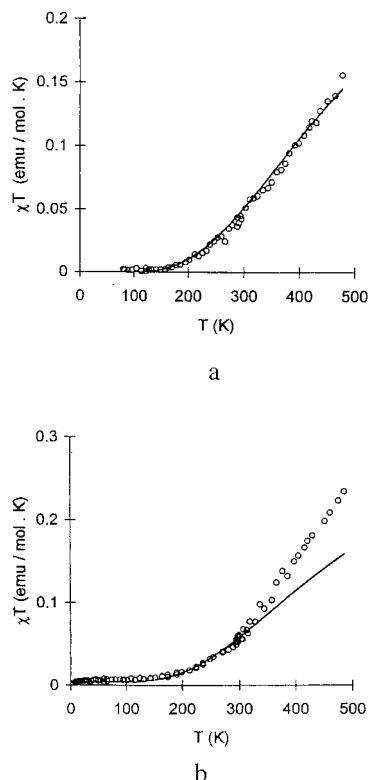


Figure 8. Temperature dependence of magnetic susceptibilities of (a) $[\text{Cu}_2\text{L}]\text{Cl}\cdot 2\text{H}_2\text{O}$ and (b) $[\text{Cu}_2\text{L}]_2[\text{Cu}_2\text{Cl}_4]$.

A standard least-squares fitting of the data for $[\text{Cu}_2\text{L}]\text{Cl}$ yielded the following values for the five parameters: $g = 2.088 \pm 0.005$, $2J = -698 \pm 10 \text{ cm}^{-1}$, $N\alpha = (59 \pm 4) \times 10^{-6} \text{ emu/mol Cu}$, $\theta = 0$, $x_p = 0$. All of the data, up to the highest measured temperature, were fitted to the above parameters. However, for the compound $[\text{Cu}_2\text{L}]_2[\text{Cu}_2\text{Cl}_4]$, only the data up to 296 K were included for fitting. A fitting analysis gave the following values for the five parameters: $g = 2.099 \pm 0.005$, $2J = -690 \pm 10 \text{ cm}^{-1}$, $N\alpha = (60 \pm 4) \times 10^{-6} \text{ emu/mol Cu}$, $\theta = (1.2 \pm 0.5) \times 10^{-3} \text{ K}$, $x_p = 0.0101 \pm 0.0005$. The curve drawn to 500 K denotes the χT behavior corresponding to the parameter values obtained above.

Even though it is evident from the crystal structure of $[\text{Cu}_2\text{L}]_2[\text{Cu}_2\text{Cl}_4]$ that two dicopper(II) cations are bound to each other, forming a dimer of dimers, no significant magnetic interaction between the dimers can be seen from the magnetic measurements (the θ -correction included in the Bleaney–Bowers equation to account for possible intradimer interactions was found to be equal to 0 for one compound and negligibly small for another one). It is possible, however, that the antiferromagnetic interaction within the dimer is too strong for any further weak interactions to be identified.

The two compounds show different behaviors at high temperatures. The experimental data for $[\text{Cu}_2\text{L}]\text{Cl}$ show a good fit to the curve calculated from the low-temperature data, with reversible susceptibility changes and no signs of decomposition. This demonstrates that the dicopper–organic ligand framework is thermally stable at least to 450 K. The behavior of the tetrachlorodicuprate(I) derivative at high temperatures is different. The experimental magnetic susceptibility above 320 K is significantly higher than that calculated from the low-temperature parameters (Figure 8b), indicating the appearance of extra spin components, and the changes at high temperature are not reversible. The measurements were conducted *in vacuo* (under 0.1 Torr of He gas), so aerial oxidation of copper(I) in the $[\text{Cu}_2\text{Cl}_4]^{2-}$ anion can be excluded. Since the dicopper–

ligand unit is stable in the chloride derivative, the initial stage of the decomposition almost certainly involves the copper(I) in the anion. Electron transfer between anionic copper(I) and copper(II) atoms in the cation could account for these observations. Formally, the spin state would be unchanged by this transition, but instead of two antiferromagnetically coupled copper(II) ions in the dicompartamental ligand, two more or less independent copper(II) ions would exist, one in the cation and one in the anion. When cooled to room temperature, samples that have been heated above 400 K show two weak and broad signals, with $g = 2.34$ and $g = 2.15$, in their EPR spectra, a behavior supporting this hypothesis. Further decomposition probably takes place, because the magnetization curve at high temperature is not completely reversible.

A comparison of the coupling constants ($2J$) for our complexes with analogous values for other Robson-type dicopper complexes show that they fall in the usual range of $2J$ values between -600 and -900 cm^{-1} .^{14,25,28,30a,34,35,38,43,46–47} (The same exchange parameter is generally referred to as $2J$, but sometimes as J ; all the numbers in this paper correspond to $2J$ in eq 1 and in the Hamiltonian $H = -2JS_1S_2$). For example, the energy separation between singlet and triplet states in the chloride derivative of the symmetrical Schiff base dicopper complex (**1** in Figure 1, $X = \text{Me}$, $Y = \text{H}$, $Z = (\text{CH}_2)_3$) has been reported to be 588,⁴⁷ 722,³⁹ or about 900 cm^{-1} .^{30b} (estimation from the data in ref 25). Despite the different estimates, it should be noted that our values for the new unsymmetrical complex are practically the same as the numbers for its symmetrical analog. This similarity can be rationalized on the basis of magnetostructural correlations.

Magnetostructural correlations have been very successful in the description of the Cu–Cu coupling in binuclear complexes with flexible noncyclic bridging ligands.^{3,50} It has been shown that the degree and even sign of this coupling is primarily determined by the Cu–O–Cu angle; if this exceeds 97.5° , an antiferromagnetic interaction is observed; if less, a ferromagnetic interaction.⁵⁰ The other significant factors are the degree of pyramidal distortion at the bridging oxygen atom (the more planar the oxygen environment, the higher the antiferromagnetic coupling), the Cu–Cu separation (not very important when a bridging ligand is involved in antiferromagnetic coupling), and the degree of coplanarity of the planes formed by each copper ion, and the two bridging oxygens (the antiferromagnetic interaction is stronger when the “halves” of the binuclear complex are coplanar).^{14,20,30,34,35,39,40,42,43,46} Since the $d_{x^2-y^2}$ orbitals of copper(II) ions are involved in the magnetic exchange pathway, it has been suggested that displacement of Cu out of the plane of the ligand will decrease the coupling constant.^{34,38,39,46}

Although the application of quantitative magnetostructural correlations to dicopper complexes with rigid macrocyclic Robson-type ligands is limited, because different structural features are not independent from each other, the same structural factors are expected to play a role in magnetic interactions. Their relative importance, however, might differ from that for acyclic complexes. For example, a decrease of the Cu–O–Cu bridging angle from 104.5° to 96.3° leads to only a modest decrease of the coupling constant (from about -800 to -689 cm^{-1})^{40,41}—in contrast with the behavior of nonrigid complexes.⁵⁰ Moreover, an attempt to correlate the J values with Cu–O(Ph)—Cu angles yielded a graph with significantly scattered data points ($R^2 = 0.52$) and with the slope of its least-squares straight line much smaller than the corresponding values for hydroxide- and

(50) Crawford, V. H.; Richardson, H. W.; Wasson, J. R.; Hodgson, D. J.; Hatfield, W. E. *Inorg. Chem.* **1976**, *15*, 2107.

alkoxide-bridged complexes.⁵¹ Significant decreases of the values of exchange constants were observed in cases of a large (0.58 Å) displacement of copper(II) out of the ligand plane (to -41 cm^{-1}),⁴³ pronounced ligand twist in a clathrochelate ligand (-66 cm^{-1}),⁴⁸ and distortion of the Cu₂O₂ fragment from planarity due to displacement of metal ions from the ligand plane to the same side of the ligand (-124 cm^{-1}).^{30a}

The various structural factors summarized above provide a foundation for considering the structure of the new dicopper Schiff base–oxime complex from the point of view of magnetic exchange coupling between the two copper ions. The dicopper complex studied here shows neither steric hindrance (which might have led to a significant twist of the ligand) nor out-of-range values for its Cu–O–Cu angles (102.3° and 103.2° for our complex, and 102.3° , 103.6° , or 104.5° for different salts of its symmetrical analog^{37,39,40}). Cu–Cu separation (3.07 Å for our complex and from 3.091 to 3.313 for different salts of a symmetrical Robson complex^{37,39,40}) and the displacement of the copper ions from their coordination planes (0.16 and 0.19 Å for our complex and from 0.019 to 0.21 Å for different salts of a Robson complex^{37,39,40}) is also similar for our Schiff base–oxime complex and its symmetrical analog ($X = \text{CH}_2$, $Y = \text{H}$, $Z = Z' = (\text{CH}_2)_3$, (Figure 1). Possible unfavorable factors include different displacements of the two kinds of Cu(II) ions from the planes of their donor atoms in the different compartments of the ligand (here 0.19 Å in the Schiff base compartment and 0.16 Å in the oxime compartment). This leads to a slight distortion of the Cu₂O₂ fragment from planarity. From the data available it is uncertain if this different displacement of Cu for different compartments is a feature of the asymmetric ligand or arises because the two copper ions have different axial ligands (chloride and oxime oxygen, respectively). The extra negative charge of the oxime ligand in comparison with the usual Robson-type ligands should also be considered. Electronic effects in symmetrical ligands either have little influence on the magnetic exchange between two copper(II) ions^{34,35,42,43} or lead to decreases in the coupling constants in the case of electron-withdrawing substituents.^{51,52} Consequently, the electron-donating properties of the oxime group can be favorable for antiferromagnetic exchange. However, the value of the antiferromagnetic interaction constant is dependent on the energy difference between the magnetic orbitals of the two copper centers; the largest overlap of magnetic orbitals will occur for two centers of the same energy,³ with the antiferromagnetic interaction decreased for two nonidentical sites. From the results of magnetic measurements it is obvious that these factors are not significant enough to decrease the magnetic coupling between two copper(II) ions. It can be concluded that the asymmetrical Schiff base–oxime ligand (**II**, Figure 1) provides an efficient pathway for magnetic interaction between two metal ions. The antiferromagnetic coupling within this binuclear cation is practically the same as that in analogous symmetrical Schiff base ligands.

Electrochemistry. Cyclic voltammograms were measured in dimethylformamide (DMF) solution for the complex [Cu₂L]Cl, as well as for the precursor mononuclear complex [CuL] (see Scheme 1). Only one reversible reduction wave with $E_{1/2} = -1.34\text{ V}$, $\Delta E = 80\text{ mV}$ was observed for the mononuclear compound. For the binuclear Schiff base–oxime complex [Cu₂L]Cl, two separate reduction waves were observed (Figure 9), with the more positive wave reversible ($E_{1/2} = -1.04\text{ V}$,

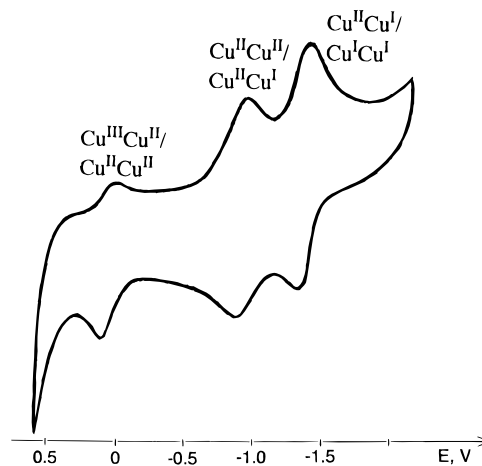
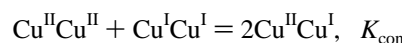


Figure 9. Cyclic voltammogram of [Cu₂L]Cl·2H₂O (10^{-3} M solution in DMF, $0.1\text{ M N}(\text{Et})_4\text{PF}_6$, scan rate 50 mV/s).

$\Delta E = 60\text{ mV}$) and the more negative wave quasi-reversible ($E_{1/2} = 1.47\text{ V}$, $\Delta E = 100\text{ mV}$); one irreversible oxidation wave is also seen (which can be quasi-reversible under certain conditions) ($E_{1/2} = +0.04$, $\Delta E = 90\text{ mV}$). Two reversible or quasi-reversible reduction waves are typical of dicopper complexes with Robson-type ligands^{14,19,20,23,27–32,35,38,40,42,43,46,53–55} and are assigned to the stepwise reduction of the copper(II) ions: the first wave corresponds to the Cu^{II}Cu^{II}/Cu^{II}Cu^I couple, and the second wave, to the Cu^{II}Cu^I/Cu^ICu^I couple. The difference between the half-wave potentials of these two processes ($\Delta E = E_{1/2}^1 - E_{1/2}^2$) is a measure of the relative stability of mixed-valent Cu^{II}Cu^I species:



$$\ln K_{\text{con}} = (nF/RT)\Delta E$$

For dicopper complexes with symmetrical ligands, the value of the comproportionation constant has been suggested as a measure of the electron delocalization in a mixed-valence complex.^{23,53} This approach obviously cannot be applied to asymmetrical complexes with two copper ions in different coordination environments. However, K_{con} still characterizes the stability of the mixed-valent complex. Despite the expectation that spin delocalization is less efficient in asymmetric complexes, the differences in half-wave potentials for the two reductions (and consequently the K_{con} values) are sometimes very high for highly distorted complexes with ligands possessing significantly different coordination sites (for a ΔE of $\sim 0.7\text{ V}$, $K_{\text{con}} \sim 10^{12} - 10^{13}$).^{19,20,30a}

The electrochemical reduction data for the asymmetrical Schiff base–oxime complex [Cu₂L]Cl can be compared with the data for an analogous symmetrical Schiff base complex (Figure 1, **I**, $X = \text{Me}$, $Y = \text{H}$, $Z = (\text{CH}_2)_3$). For the latter compound, the half-wave potentials measured in the same solvent (DMF) were reported to be -1.31 and -0.92 V ; $\Delta E = 0.39\text{ V}$.²³ Both potentials are more negative for the oxime-containing ligand, which can be attributed to the stabilization of the higher oxidation state (and destabilization of the lower oxidation state) by the additional negative charge on the ligand. This behavior, while consistent with the electrochemistry of copper oxime complexes,^{56,57} differs from that reported by Addison⁵⁴ who found that potentials are practically the same

(51) Thompson, L. K.; Mandal, S. K.; Tandon, S. S.; Bridson, J. N.; Park, M. K. *Inorg. Chem.* **1996**, *35*, 3117.

(52) MacLachlan, M. J.; Park, M. K.; Thompson, L. K. *Inorg. Chem.* **1996**, *35*, 5492.

(53) Gagné, R. R.; Spiro, C. L. *J. Am. Chem. Soc.* **1980**, *102*, 1443.

(54) Addison, A. W. *Inorg. Nucl. Chem. Lett.* **1976**, *12*, 899.

(55) Mandal, S. K.; Adhikary, B.; Nag, K. *J. Chem. Soc., Dalton Trans.* **1986**, 1175.

Table 3. Atomic Coordinates ($\times 10^4$) and Equivalent Isotropic Displacement Parameters ($\text{\AA}^2 \times 10^3$) for $[\text{Cu}_2\text{L}]_2^+[\text{Cu}_2\text{Cl}_4]^{2-}$ (A)

	x	y	z	$U(\text{eq})^a$
Cu(1)	130.4(4)	4246.6(3)	3840.9(2)	24(1)
Cu(2)	-1263.5(4)	4426.0(3)	2131.7(2)	26(1)
Cu(3)	205.2(8)	1424.7(6)	617.3(3)	64(1)
Cl(1)	-2160.7(12)	192.9(12)	-173.7(6)	57(1)
Cl(2)	1296.2(10)	3461.4(10)	1509.1(5)	43(1)
O(1)	1441(3)	2503(2)	4986.3(12)	41(1)
N(2)	302(3)	2357(3)	4326.9(12)	28(1)
C(3)	-575(4)	902(3)	4084(2)	32(1)
C(4)	-1849(3)	378(3)	3403.3(15)	27(1)
C(5)	-2178(3)	1359(3)	2840.5(14)	24(1)
O(6)	-1390(2)	2929(2)	2931.4(10)	26(1)
C(7)	-3377(3)	620(3)	2179(2)	28(1)
C(8)	-3839(4)	1462(3)	1551(2)	32(1)
N(9)	-3226(3)	2931(3)	1454.5(13)	30(1)
C(10)	-3996(4)	3401(4)	735(2)	43(1)
C(11)	-2673(5)	4512(4)	330(2)	46(1)
C(12)	-2077(6)	6166(4)	766(2)	59(1)
N(13)	-1079(3)	6285(3)	1551.0(14)	35(1)
C(14)	-97(4)	7691(3)	1796(2)	37(1)
C(15)	1005(4)	8258(3)	2533(2)	29(1)
C(16)	1121(3)	7322(3)	3148.1(14)	25(1)
O(17)	198(2)	5788(2)	3077.5(10)	28(1)
C(18)	2233(3)	8072(3)	3840(2)	28(1)
C(19)	2492(3)	7288(3)	4530(2)	30(1)
N(20)	1784(3)	5817(3)	4611.1(12)	27(1)
O(21)	2112(3)	5394(2)	5347.8(11)	33(1)
C(22)	-2754(4)	-1255(3)	3310(2)	34(1)
C(23)	-3969(4)	-1979(3)	2678(2)	34(1)
C(24)	-4928(5)	-3727(3)	2625(2)	47(1)
C(25)	-4247(4)	-1023(3)	2116(2)	35(1)
C(26)	1946(4)	9889(3)	2622(2)	35(1)
C(27)	3012(4)	10636(3)	3298(2)	34(1)
C(28)	3962(4)	12397(3)	3386(2)	45(1)
C(29)	3135(4)	9701(3)	3895(2)	34(1)

^a $U(\text{eq})$ is defined as one-third of the trace of the orthogonalized U_{ij} tensor.

for complexes of ligands with $X = \text{Me}$, $Y = \text{Me}$, $Z = (\text{CH}_2)_3$ and $X = \text{Me}$, $Y = \text{Me}$, $Z = \text{OBF}_2\text{O}^-$; he concluded that the negative charge of the ligand does not influence the reduction potential of the copper complex. However, this result can also be explained by the shift to more positive redox potentials for copper complexes with BF_2 -bridged oxime ligands compared to simple copper oximes.⁵⁶

Structural variation in dicopper complexes with Robson-type ligands causes a variety of effects in their electrochemical behavior. For example, changes in the Y substituents (**I**, Figure 1) lead to significant changes in the second (more negative) redox potential, but not the first potential.²⁷ On the other hand, reduction of azomethine bonds and variations in the lengths of the polymethylene chains Z in the reduced ligands lead to variations in the first, but not the second, potential.^{30b} In our complex, introduction of negatively charged Z ($\text{O}-\text{H}-\text{O}^-$ instead of $(\text{CH}_2)_3$) in one compartment of the ligand leads to negative shifts in the redox potential of the copper in both compartments. The stability of the mixed-valence species is quite high ($\Delta E = 0.43 \text{ V}$, $K_{\text{con}} = 1.9 \times 10^7$), slightly higher than the stability of the $\text{Cu}^{\text{II}}\text{Cu}^{\text{I}}$ complex in the symmetrical Schiff base analog ($\Delta E = 0.39 \text{ V}$, $K_{\text{con}} = 5.6 \times 10^5$).²³

Previously reported alterations in Robson-type dicopper complexes extended the range of redox potentials in the positive direction,^{35,42-43} particularly targeting materials with spin exchange along infinite cation-anion chains.³⁵ Our results show that the range of redox potentials can be extended in the negative

direction by introducing negatively charged oxime groups into the ligand, without loss of stability of the mixed-valent $\text{Cu}^{\text{II}}\text{Cu}^{\text{I}}$ complex.

An interesting feature in the electrochemical behavior of $[\text{Cu}_2\text{L}]\text{Cl}$ is the presence of an oxidation wave $+0.04 \text{ V}$. This wave is irreversible when CVA is registered in the range $+0.6$ to -2.1 V . However, it becomes quasi-reversible for scans from $+0.6$ to -0.6 V and then back (scan rate 50, 100, or 200 mV/s). This one-electron oxidation wave can be tentatively assigned to $\text{Cu}^{\text{II}}\text{Cu}^{\text{II}}-\text{Cu}^{\text{III}}\text{Cu}^{\text{II}}$ oxidation, with oxidation of the $\text{Cu}(\text{II})$ in the oxime compartment. The potential of this process is significantly lower than the oxidation potential of dicopper complexes with amine dicompartmental ligands,²⁸ reflecting the ability of oxime ligands to stabilize high oxidation states. Thus, for $\text{Cu}(\text{dmgH})_2$ ($\text{dmgH} = \text{dimethylglyoximate}$) in CH_2Cl_2 the following potentials have been reported: $+0.38 \text{ V}$ (oxidation), -1.26 V (reduction)⁵⁷ (potentials recalculated *vs* Fc^+/Fc). For these two processes $\Delta E = 1.64 \text{ V}$, compared to 1.51 V for the oxime compartment of our complex, supporting the suggested assignment of this oxidation wave.

Conclusions

A new strategy has been suggested for building chains of magnetically coupled metal ions in which binuclear complexes are designed so that they can be bound to each other by a fifth metal ion. As building blocks for such a strategy, dicopper(II) complexes have been synthesized and characterized with an asymmetric Robson-type ligand, consisting of Schiff base and oxime compartments. X-ray structure determination shows that the asymmetry of the dicompartmental ligand does not introduce significant distortion of the planar structure of binuclear cations, with Cu-donor atom bond lengths and angles close to those for analogous symmetrical Robson complexes. As a result, a strong antiferromagnetic interaction (*ca.* -700 cm^{-1}) between two copper(II) centers exists within the binuclear cations. Cyclic voltammograms of the newly synthesized complexes show one oxidation and two reduction waves, with relative stabilization of higher oxidation states of copper. The two consecutive reduction waves are significantly separated from each other (by 430 mV), making mixed-valent $\text{Cu}^{\text{II}}\text{Cu}^{\text{I}}$ species thermodynamically stable toward disproportionation. As anticipated for this design, the oxime oxygens show significant tendencies to be coordinated to other metal ions. In the absence of a fifth metal, they coordinate axially to the copper ions from other binuclear cations. This results in the formation of the coordination tetramers (for the perchlorate salt) or coordination polymers (for the $[\text{Cu}_2\text{Cl}_4]^{2-}$ salt, where the unusual anions provide additional bridging possibilities). Consequently, the dicopper complexes with the new unsymmetrical dicompartmental ligand retain the main advantages of symmetric Robson complexes (strong magnetic coupling and stabilization of mixed-valent species) and add the potential to extend the number of metal ions coordinated with it and coupled to each other. The syntheses of heterodinuclear complexes with this dicompartmental ligand and pentanuclear complexes resulted from their interaction with the fifth metal ion, as well as their cryomagnetic studies, are currently in progress in our laboratories.

Experimental Section

Electronic absorption spectra were recorded on a Varian Model 2300 recording spectrophotometer. IR spectra were obtained from KBr disks using a Perkin-Elmer Model 1600 Fourier transform spectrometer. ESR spectra were measured using a Bruker ESP 300 E ESR spectrometer,

(56) Gagné, R. R.; Allison, J. L.; Gall, R. S.; Koval, C. A. *J. Am. Chem. Soc.* **1977**, *99*, 7170.

(57) Chaudhuri, P.; Winter, M.; Della Vedova, B. P. C., et al. *Inorg. Chem.* **1991**, *30*, 2148.

Table 4. Atomic Coordinates ($\times 10^4$) and Equivalent Isotropic Displacement Parameters ($\text{\AA}^2 \times 10^3$) for $[\text{Cu}_2\text{L}]^+[\text{ClO}_4]^- \cdot \text{MeOH}$ (B)

	x	y	z	$U(\text{eq})^a$		x	y	z	$U(\text{eq})^a$
Cu(11)	157.2(13)	9372.7(7)	728.4(5)	38(1)	C(208)	-1703(11)	4690(7)	4244(5)	54(3)
Cu(12)	1235.8(13)	9568.2(7)	2348.0(5)	39(1)	N(209)	-1067(9)	4331(5)	3702(4)	53(2)
O(101)	-1821(7)	9508(4)	-513(3)	44(2)	C(210)	-819(16)	3413(7)	3618(7)	93(4)
N(102)	-1676(8)	9665(4)	221(4)	38(2)	C(211)	218(19)	3091(8)	3177(7)	111(5)
C(103)	-2733(10)	10074(5)	530(5)	39(2)	C(212)	188(15)	3091(6)	2453(5)	73(3)
C(104)	-2811(11)	10349(6)	1292(5)	43(2)	N(213)	207(9)	3966(4)	2329(4)	45(2)
C(105)	-1643(10)	10271(5)	1848(4)	34(2)	C(214)	751(11)	4033(6)	1764(5)	46(2)
O(106)	-363(7)	9898(4)	1695(3)	39(2)	C(215)	979(10)	4780(5)	1489(5)	37(2)
C(107)	-1893(11)	10589(5)	2583(5)	41(2)	C(216)	586(10)	5602(6)	1813(5)	37(2)
C(108)	-814(12)	10561(6)	3194(5)	49(3)	O(217)	-58(6)	5771(3)	2431(3)	38(1)
N(109)	454(10)	10240(5)	3222(4)	47(2)	C(218)	887(10)	6300(6)	1501(5)	37(2)
C(110)	1218(14)	10271(9)	3951(5)	93(4)	C(219)	553(10)	7199(6)	1785(5)	43(2)
C(111)	2910(14)	10317(8)	4038(6)	86(4)	N(220)	-128(8)	7503(4)	2318(4)	40(2)
C(112)	3607(12)	9571(7)	3627(5)	67(3)	O(221)	-340(7)	8380(4)	2455(3)	52(2)
N(113)	3248(9)	9385(5)	2836(4)	45(2)	C(222)	-3501(11)	7056(6)	4943(5)	48(3)
C(114)	4321(12)	9052(6)	2500(5)	47(2)	C(223)	-3675(11)	6436(7)	5310(5)	48(3)
C(115)	4312(11)	8722(5)	1718(5)	41(2)	C(224)	-4526(12)	6591(7)	5963(5)	67(3)
C(116)	3041(11)	8715(5)	1179(5)	39(2)	C(225)	-3036(11)	5674(6)	5053(5)	48(2)
O(117)	1793(6)	9078(3)	1375(3)	34(1)	C(226)	1625(10)	4661(6)	854(5)	44(2)
C(118)	3122(10)	8271(5)	454(5)	36(2)	C(227)	1921(10)	5297(6)	524(5)	43(2)
C(119)	1849(11)	8109(6)	-157(5)	46(2)	C(228)	2680(12)	5156(7)	-137(5)	60(3)
N(120)	609(9)	8469(4)	-125(3)	39(2)	C(229)	1539(10)	6113(6)	862(5)	46(2)
O(121)	-437(8)	8201(4)	-768(3)	55(2)	O(1S)	2051(8)	5561(4)	3773(3)	65(2)
C(122)	-4109(10)	10739(6)	1490(5)	44(2)	C(1S)	3377(13)	5594(8)	3426(6)	83(4)
C(123)	-4394(12)	11039(6)	2192(6)	49(3)	O(2S)	-3270(8)	6134(5)	2045(4)	81(2)
C(124)	-5861(12)	11427(7)	2353(5)	66(3)	C(2S)	-4712(14)	6325(8)	1986(8)	107(5)
C(125)	-3237(12)	10962(6)	2727(5)	47(2)	Cl(1)	4432(4)	6302(2)	8181(2)	64(1)
C(126)	5658(11)	8356(6)	1514(5)	45(2)	O(11)	3745(10)	7072(5)	8373(5)	112(3)
C(127)	5755(11)	7949(6)	792(6)	47(2)	O(12) ^b	5274(31)	6182(17)	8800(10)	133(14)
C(128)	7197(11)	7541(7)	587(6)	69(3)	O(13) ^b	5364(46)	6322(19)	7678(17)	215(24)
C(129)	4477(11)	7919(6)	284(5)	49(2)	O(14) ^b	3194(21)	5573(9)	7910(19)	146(16)
Cu(21)	-979.0(13)	6812.0(7)	2907.7(6)	38(1)	O(12A) ^c	4220(58)	5776(23)	8628(17)	168(22)
Cu(22)	-493.3(13)	4957.1(7)	3010.6(6)	42(1)	O(13A) ^c	6015(21)	6594(26)	8210(26)	182(23)
O(201)	-2175(9)	8497(4)	3308(4)	60(2)	O(14A) ^c	3763(32)	5812(27)	7466(11)	129(15)
N(202)	-2001(8)	7731(4)	3490(4)	40(2)	Cl(2)	2181(4)	7962(2)	4807(2)	72(1)
C(203)	-2672(10)	7677(6)	4030(5)	43(2)	O(21)	1938(13)	7665(6)	4059(5)	137(4)
C(204)	2739(10)	6943(6)	4346(4)	37(2)	O(22)	2231(16)	7212(8)	5011(6)	204(6)
C(205)	-2061(10)	6166(6)	4086(5)	42(2)	O(23)	3539(12)	8503(7)	5081(7)	196(6)
O(206)	-1354(6)	6032(3)	3516(3)	37(1)	O(24)	977(13)	8366(10)	5006(6)	251(9)
C(207)	-2227(11)	5528(6)	4456(5)	44(2)					

^a $U(\text{eq})$ is defined as one-third of the trace of the orthogonalized U_{ij} tensor. ^b Occupancy 0.58(3). ^c Occupancy 0.42(3).

Table 5. Atomic Coordinates ($\times 10^4$) and Equivalent Isotropic Displacement Parameters ($\text{\AA}^2 \times 10^3$) for $[\text{Cu}(\text{L}2)_2]$ (C)

	x	y	z	$U(\text{eq})^a$
Cu(1)	5000	5000	0	42(1)
O(1)	3279(3)	3533(3)	917(4)	69(1)
N(2)	4305(3)	4010(3)	1487(5)	48(1)
C(3)	4666(3)	3723(4)	3004(6)	48(1)
C(4)	5698(3)	4103(3)	3864(5)	43(1)
C(5)	6366(3)	4920(4)	3198(5)	41(1)
O(6)	6112(2)	5390(3)	1706(4)	50(1)
C(7)	7355(3)	5253(3)	4178(5)	44(1)
C(8)	8048(3)	6123(4)	3449(5)	44(1)
O(9)	8914(2)	6433(3)	4668(4)	57(1)
O(10)	8439(2)	5766(3)	1951(4)	48(1)
C(11)	9056(4)	4740(5)	2125(7)	69(2)
C(12)	7646(4)	4784(4)	5739(6)	50(1)
C(13)	6998(4)	3968(4)	6412(6)	52(1)
C(14)	6035(3)	3657(4)	5467(5)	47(1)
C(15)	7353(4)	3477(5)	8132(6)	69(2)
C(16)	9513(4)	7388(5)	4193(6)	70(2)

^a $U(\text{eq})$ is defined as one-third of the trace of the orthogonalized U_{ij} tensor.

with diphenylpicrylhydrazyl (DPPH) as a standard. Fast atom bombardment (FAB) mass spectra were obtained in matrices of magic bullet and nitrobenzyl alcohol, with argon as a fast atom beam. Cyclic voltammetry (CVA) was performed using a three-electrode system consisting of a glassy carbon working electrode, platinum auxiliary electrode, and silver reference electrode. Voltammograms were recorded with a Princeton Applied Research Model 173 potentiostat,

fitted with a Model 179 digital coulometer and a Princeton Applied Research Model 175 Universal programmer. The scan rate range was 50–200 mV/s, with all measurements performed in 2×10^{-3} M DMF solutions containing 0.1 M tetrabutylammonium hexafluorophosphate as a supporting electrolyte. Ferrocene was used as an internal standard, and all potentials are quoted versus the Fc^+/Fc couple.

Room temperature magnetic moments were measured using a Johnson Matthey magnetic susceptibility balance calibrated with mercury tetrathiocyanatocobaltate(II). Cryomagnetic studies used a "force magnetometer" in an external magnetic field of 5 kG, which has previously been described.⁵⁸

All chemicals were of reagent grade. 2,6-Diformyl-4-methylphenol was synthesized as described in ref 59, and the monocopper complex with ligand L1 (Scheme 1), according to ref 23.

Synthesis of $[\text{Cu}_2\text{L}]\text{Cl} \cdot 2\text{H}_2\text{O}$. To 0.125 g of $[\text{CuL}1]$ suspended in 10 mL of methanol was added with stirring 0.050 g (1 equiv) of $\text{CuCl}_2 \cdot 2\text{H}_2\text{O}$; a clear brown-green solution was formed in 20 min. To this solution 0.040 g (2 equiv) of $\text{NH}_2\text{OH} \cdot \text{HCl}$ was added, followed by 0.12 mL (3 equiv) of triethylamine. The mixture was stirred at ambient temperature for 30 min, when a green precipitate appeared. After stirring overnight, the green precipitate was removed by filtration or centrifugation. The precipitate was washed with small portions of methanol, followed by ether, and dried under vacuum; yield, 0.083 g (48%; 67% for a preparation at 10-fold scale). The compound can be recrystallized from methanol. MS (positive FAB, methanol–NBA): 519, 521 ($[\text{Cu}_2\text{L}]^+$). IR (medium and strong bands only): 3417 (broad),

(58) Kahol, P. K.; McCormick, B. J. *J. Phys.: Condens. Matter* **1991**, *3*, 7963.

(59) Ullmann, F.; Brittner, K. *Berichte* **1909**, *42* (B.II), 2539.

2923, 1629, 1564, 1479, 1455, 1421, 1386, 1310, 1284, 1235, 1192, 1113, 1096, 1071, 813, 760, 645, 568, 516 cm^{-1} . Anal. Calcd for $\text{C}_{21}\text{H}_{25}\text{N}_4\text{O}_6\text{Cu}_2\text{Cl}$: C, 42.61; H, 4.26; N, 9.46; Cu, 21.47. Found: C, 43.17; H, 4.20; N, 9.20; Cu, 21.63.

Isolation of $[\text{Cu}(\text{L}_2)_2]$. On allowing the filtrate from the synthesis of $[\text{Cu}_2\text{L}]\text{Cl}$ to stand overnight in an open flask, a brown-green solid crystallized. Filtration and careful washing with methanol gave $[\text{Cu}(\text{L}_2)_2]$ as a brown crystalline solid; yield, about 5%. MS (positive FAB, CHCl_3 -NBA): 510, 512 (molecular ion); 480; 448. IR (medium and strong bands only): 3430 (broad), 3198, 2987, 2934, 2825, 1682 (w), 1627, 1558, 1456, 1444, 1370, 1290, 1253 (w), 1228, 1194, 1118, 1047, 1025, 999, 887, 863, 804, 700, 668, 619, 570, 531 cm^{-1} .

Synthesis of $[\text{Cu}_2\text{L}][\text{Cu}_2\text{Cl}_4]$. A small amount of this compound crystallizes out of the filtrate and the methanol washings in the synthesis of the chloride salt. A better yield is achieved by using an excess of copper chloride and hydroxylamine in the chloride synthesis. After mixing 1 equiv of $[\text{CuL}1]$, 1 equiv of $\text{CuCl}_2 \cdot 2\text{H}_2\text{O}$, 2 equiv of $\text{NH}_2\text{OH} \cdot \text{HCl}$, and 3 equiv of NEt_3 in methanol, the mixture was stirred for several minutes until the precipitate started to form. At this stage, 1 equiv (0.050 g) of $\text{CuCl}_2 \cdot 2\text{H}_2\text{O}$ was added, followed by 0.5 equiv of $\text{NH}_2\text{OH} \cdot \text{HCl}$. After the mixture was stirred for 30 min, a brown-green precipitate separated from the solution. This was redissolved in 20 mL of methanol, undissolved brown precipitate centrifuged off, and the solvent evaporated slowly in air. The diamond-shaped crystals of the tetrachlorodocuprate(I) salt were filtered, washed with a small amount of ethanol and with ether, and dried under vacuum; yield, 0.042 g (22%). MS (positive FAB, methanol-NBA): 519, 521 ($[\text{Cu}_2\text{L}]^+$). IR (medium and strong bands only): 3393 (broad), 2923, 1628, 1594, 1567, 1455, 1419, 1304, 1275, 1237, 1192, 1115, 1097, 1068, 1002, 812, 758, 645 cm^{-1} . Anal. Calcd for $\text{C}_{42}\text{H}_{42}\text{N}_8\text{O}_8\text{Cu}_6\text{Cl}_4$: C, 38.51; H, 3.23; N, 8.55; Cu, 29.11. Found: C, 38.93; H, 3.45; N, 8.71; Cu, 28.44.

Synthesis of $[\text{Cu}_2\text{L}](\text{ClO}_4) \cdot \text{MeOH}$. *Caution: Perchlorates are potentially explosive.* A 0.1 g amount of $[\text{Cu}_2\text{L}]\text{Cl} \cdot 2\text{H}_2\text{O}$ was dissolved in a minimum amount of methanol (about 30 mL). A solution of 0.20 g of $\text{NaClO}_4 \cdot \text{H}_2\text{O}$ in 5 mL of methanol was added. A dark green precipitate started to form immediately. The mixture was kept for 1 h; then the microcrystalline precipitate was filtered, washed with small amounts of methanol and ether, and dried in air; yield, 0.080 g (70%). X-ray quality crystals were obtained by a similar procedure, but an equivalent amount of sodium perchlorate was added to the dilute methanol solution of $[\text{Cu}_2\text{L}]\text{Cl} \cdot 2\text{H}_2\text{O}$. Slow evaporation of the solvent resulted in crystal formation. MS (positive FAB, methanol-NBA): 519, 521. IR (medium and strong bands only): 3446 (broad), 3013,

2922, 2861, 1634, 1595, 1568, 1456, 1419, 1387, 1309, 1272, 1240, 1196, 1090 (very strong), 994, 940, 876, 813, 758, 625, 572, 518 cm^{-1} .

Crystal Structure Analysis. Crystal data are given in Table 1 for compounds **A**–**C**. Crystals of **A** were well-formed dark brown plates, green in transmitted light; for **B**, small brown blocks; for **C**, dark brown plates.

(A) Data Collection and Processing. Siemens P3R3 (P4 for **A**) four-circle diffractometer, $\lambda = 0.71073 \text{ \AA}$, ω - 2θ mode, with scan range of $\pm 1.0 (2\theta)$ around the $K_{\alpha 1} - K_{\alpha 2}$ angles, scan speed 3–29 deg min^{-1} , depending upon the intensity of the 2 s prescan; backgrounds measured at each end of the scan for 0.25 of the scan time. Cell constants obtained by least-squares refinement on diffractometer angles for 15 (30 for **A**) automatically centered reflections. Three standard reflections were monitored every 200 reflections and showed no decrease during data collection. Reflections were corrected for absorption effects by the Gaussian method for **A** and by the analytical method using ABSPSI for **C**;⁶⁰ no correction for **B**.

(B) Structure Analysis and Refinement. For **A**, heavy atoms were located by the Patterson interpretation section of SHELXTL PLUS⁶¹ and the light atoms then found by E-map expansion and successive Fourier syntheses; **B** and **C** were solved by direct methods using SHELXTL PLUS⁶¹ (TREF). Hydrogen atoms were added at calculated positions and refined using a riding model. For **A**, the oxime-hydrogen was not located. Anisotropic displacement parameters were used for all non-H atoms; H atoms were given isotropic displacement parameters $U = 0.08 \text{ \AA}^2$. The weighting scheme was $w_{\text{calc}} = 1/[\sigma^2(F_o^2) + (aP)^2 + bP]$, where $P = (F_o^2 + 2F_c^2)/3$. Refinement used SHELXTL-93.⁶²

For **A**, the large difference peak and hole, +2.041 and $-1.337 \text{ e \AA}^{-3}$, lie close to Cu(3) and probably represent an unresolved disorder of the bridging group. For **B**, three oxygen atoms of one perchlorate group were disordered (occupancies 0.58(3) and 0.42(3); Cl–O and O–O distances were restrained to approximate equality). For **C**, the structure solution revealed a centrosymmetric structure with Cu on an inversion center. Selected bond lengths and angles in Table 2, and atomic coordinates are given in Tables 3–5.

Acknowledgment. This material is based upon work supported by the NSF under EPSCoR Grant OSR-9255223. The government has certain rights in this material. This work also received matching support from the state of Kansas. We would like to thank the reviewers for careful reviewing of our manuscript.

Supporting Information Available: Tables listing full bond lengths and angles, thermal parameters, and H-atom coordinates, and complete information on crystal data, collection, and refinement parameters (27 pages). Ordering information is given on any current masthead page.

IC9601145

(60) Alcock, N. W.; Marks, P. J. *J. Appl. Crystallogr.* **1993**, *27*, 200.

(61) Sheldrick, G. M. *SHELXTL PLUS user's manual*; Nicolet Instrument Co.: Madison, WI, 1986.

(62) Sheldrick, G. M. *J. Appl. Crystallogr.*, in press.